INFECTION AND IMMUNITY, Oct. 2005, p. 6962–6973 Vol. 73, No. 10
0019-9567/05/$08.00+0 doi:10.1128/IAI.73.10.6962–6973.2005

Expression of Matrix Metalloproteinases Subsequent to Urogenital *Chlamydia muridarum* Infection of Mice

K.H. Ramsey,* I.M. Sigar, J. H. Schripsema, N. Shaba, and K. P. Cohoon

Department of Microbiology and Immunology, Chicago College of Osteopathic Medicine, Midwestern University, Downers Grove, Illinois 60515

Received 24 March 2005/Returned for modification 2 May 2005/Accepted 30 May 2005

The central hypothesis of this study was that matrix metalloproteinases (MMPs) would be enhanced following murine chlamydial infection and that their expression would vary in mouse strains that differ in their susceptibility to chronic chlamydia-induced disease. To address this hypothesis, female C3H/HeN and C57BL/6 mice were infected intravaginally with *Chlamydia muridarum*. Uterine and oviduct tissues were assessed for transcription of MMP genes and their tissue inhibitors. An increased activity of MMP genes relative to preinfection tissues was observed in the C3H/HeN mice when compared to C57BL/6 mice. Using gelatin zymography, we detected constitutive MMP-2 activity in both strains of mice but an increase in MMP-9. Casein zymography indicated the presence of two elastase-like activities consistent with MMP-12 and possibly MMP-7. Western blotting and antigen capture enzyme-linked immunoassay also confirmed an increase in MMP-9 but constitutive MMP-2 expression subsequent to the infection in both strains of mice. In C57BL/6 mice, MMP-9 was present in monomer and dimer form throughout the 56-day monitoring period. C3H/HeN mice produced dimeric MMP-9, but increases in the monomer form were also observed through day 14. Post-translational modification of MMP-9 between the two strains also differed. Immunohistochemistry revealed neutrophils as a prominent source for MMP-9 in both strains of mice. We conclude that differences in the relative expression and activity of MMPs, particularly MMP-9, occur in mice differing in their susceptibility to the development of chronic chlamydial disease. These differences may account for disparate outcomes with regard to chronic sequelae of the disease.

Mouse strains have been characterized into susceptible or resistant phenotypes based on a variety of outcomes following chlamydial infection, regardless of the chlamydial strain or infection routes used. In lung and intraperitoneal infections, susceptibility is based on lethality and pathology (4, 53). In urogenital infection, disease outcomes assessed have been tubal scarring (39, 40), infertility (7, 11, 43), histopathology or gross pathology (7, 39), and infection course (7). Despite the variations in parameters of chlamydial strain and outcomes assessed, the phenotypes remain constant in urogenital tract infections. C3H/HeN (*H-2*^{k}) mice are classified as susceptible, BALB/c (*H-2*^{d}) mice as moderately susceptible, and C57BL/6 (*H-2*^{b}) mice as resistant. In murine lung infections with *Chlamydia psittaci*, the disease may take on a completely different pattern of susceptibility and this may reflect differences in immune effectors at distinct anatomical sites (17). The importance of these strain differences lies in the opportunity to compare host responses between strains and subsequently identify the risks of adverse infection outcome and subsequent chronic chlamydial disease.

Hydrosalpinx formation, infertility, and fibrotic oviduct occlusion are routine consequences of infection following a single urogenital inoculation of *Chlamydia muridarum* (previously, the mouse pneumonitis strain of *Chlamydia trachomatis*, MoPn) in susceptible mouse strains, though these sequelae also occur in resistant strains at a lower rate (7, 11, 39, 40). Tumor necrosis factor alpha and interleukin 1β (IL-1β) levels are markedly elevated in the C57BL/6 mice relative to C3H/HeN mice, and there are correlative data related to a prolonged presence of neutrophils and coincident increases in chemokine macrophage inflammatory protein 2 in the susceptible strains (8, 9). Apoptosis and Toll-like receptor 2 signaling have both also been implied in initiating and regulating inflammatory damage in this model (10, 32). Cumulatively, these data indicate that variances in the innate response to the infection are likely to be associated with adverse infection outcomes in this model.

We have found that nitrogen and oxygen radicals interact to have a major influencing role on pathogenesis in this model (35, 36). In the absence of phagocyte oxidase, mice are spared the chronic sequelae of hydrosalpinx and infertility following chlamydial infection whereas the loss of inducible nitric oxide synthase significantly increases the rate of chronic sequelae. Interestingly, oxygen and nitrogen radicals have likewise been shown to have opposing regulatory effects on host enzymes that influence the degradation of the extracellular matrix (ECM) (23, 28, 31). The matrix metalloproteinases (MMPs) are a class of zinc-dependent proteinases that are involved in the proteolysis and resynthesis of the ECM (21, 29), processing of cytokines to active forms as well as the release of sequestered growth and signaling factors (15, 27, 30), and chemotaxis and migration of leukocytes through inflamed tissues (30, 44, 45). Dysregulation of MMPs has been attributed to diseases such as atherosclerosis, angiogenesis, tumor growth and metastasis, rheumatoid arthritis and other autoimmune disorders, and chronic fibrotic diseases as reviewed in references 12, 37, and 38). Hence, many factors (nitrogen and oxygen radicals,

* Corresponding author. Mailing address: Department of Microbiology, Chicago College of Osteopathic Medicine, Midwestern University, 555 31st Street, Downers Grove, IL 60516. Phone: (630) 515-6165. Fax: (630) 515-7245. E-mail: kramse@midwestern.edu.

chemokine and cytokine expression patterns, etc.) may alter the expression or activity of MMPs during an inflammatory event and altered MMP activity may, in turn, influence the turnover of the ECM by either suppressing or enhancing excessive ECM production (i.e., fibrosis). With regard to chlamydial infections, a role for MMP has also been proposed in trachoma (1, 2) and enhanced MMP expression has been reported in an in vitro model of human fallopian tube infection (3).

In the present study, as a first step toward delineating possible differences in MMP activity in mouse strains that differ in their susceptibility to chronic chlamydial disease, we assessed the production of MMPs and their natural tissue inhibitors (TIMPs) on the transcriptional, translational, and post-translational levels subsequent to MoPn urogenital infection. This was accomplished by using mini-gene arrays, gelatin and casein zymography, antigen capture enzyme-linked immunoassay (EIA), and Western blotting.

MATERIALS AND METHODS

Mice and infection. Five- to six-week-old female C3H/HeN or C57BL/6 mice were obtained from Harlan Sprague-Dawley (Indianapolis, Indiana) and housed with rodent chow and water ad libitum with a 12:12 light/dark cycle. After a 10-day acclimation period, mice were pretreated with 2.5 mg of medroxyprogesterone acetate (DepoProvera P4; Upjohn, Kalamazoo, Mich.) and 7 days later inoculated intravaginally with 200 50% infective doses (10^4 inclusion-forming units [IFU]) of HeLa 229-grown *C. muridarum*, MoPn, exactly as described elsewhere (6). For controls, some mice were pretreated with progesterone and not infected and in one experiment, progesterone pretreatment was omitted prior to infection. In order to verify infection, cervical-vaginal swabs were collected in all mice at day 4 postinfection and the infection course was followed in a subset of mice at 4, 7, 10, 14, 21, 28, and 35 days postinfection. *C. muridarum* was isolated and quantified in HeLa 229 cultures as previously described (6).

Transcriptional profiling of MMP and TIMP genes in response to MoPn infection. At analogous time points postinfection as with the cervical-vaginal swabs described above, a subset of mice was euthanized by cervical dislocation while under ketamine-xylazine anesthesia. The sampling times were selected to be representative of preinfection (day 0), peak infection (days 4 to 14), infection nadir (days 21 to 28), immediate postinfection (day 35), and resolution of inflammation but with chronic disease sequelae (day 56). The upper uterus and oviduct (excluding ovary, lower uterus, and cervix) were placed in Trizol reagent (Invitrogen, Carlsbad, CA) on ice and homogenized using a handheld power homogenizer (Tissue-Terror; Biospec Products, Inc., Bartlesville, OK). RNA was extracted according to the manufacturer's specifications, and purity and intactness of the transcripts were verified on 1.5% agarose gels. The contralateral upper uterus and oviduct were placed in cold phosphate-buffered saline (PBS) at pH 7.2, homogenized, and processed for protein content, for zymography, and for Western blot analysis as described below. Following the nonradioactive mouse matrix metalloproteinase GEArray protocols (SuperArray Inc., Bethesda, MD), 5 μg of total RNA was reverse transcribed in the presence of biotinylated nucleotides to create cDNA probes representing expressed genes from the murine tissue. These were then hybridized to gene-specific cDNA fragments spotted in duplicate on nylon membranes. The membranes were blocked and incubated with alkaline phosphatase-conjugated streptavidin and washed, and the relative expression levels for targeted genes were detected using a chemiluminescence developer supplied by the manufacturer. All films were exposed for 5 min using Kodak X-Omat AR film (Kodak, Inc., Rochester, NY), scanned (Hewlett-Packard Scanjet 7400c), and analyzed using SigmaGel, version 1.0, software (Gandel Corp., San Rafael, CA). Localized background was subtracted from all spots, and duplicate spots were averaged. Relative signal strength for each membrane was determined by expressing all genes as a ratio of the average of the housekeeping genes beta actin and glyceraldehyde-3-phosphate dehydrogenase (GAPDH). An average density of spots for each gene was taken for four to six tissue samples each derived from separate mice for two or three experiments. For semiquantitative comparisons, values were expressed relative to day 0 which were taken to be baseline activity for that gene. In addition, several trial runs were conducted to compare and control for the effects of estrus cycle (animals with no infection but which were followed in parallel time points with infected animals) and P4 treatment (animals with no P4 pretreatment but which were inoculated and followed in parallel with P4-pretreated mice). In summary, it was found that P4 tends to moderately suppress background (day 0) MMP-2 and MMP-9 expression but otherwise had no discernible effect on the overall results observed for MMP expression subsequent to infection.

Zymography. At the time of specimen collection for RNA isolation and transcriptional profiling as described above, the contralateral upper uterus and oviduct were excised and homogenized in cold PBS (pH 7.2). The homogenate was cleared of debris by centrifugation at 800 × *g* for 10 min at 4°C, and the supernatant was frozen in aliquots at −70°C. Total protein content was determined by the bicinchoninic acid method (Pierce BCA; Pierce-Endogen, Rockford, IL), and loading amounts were standardized to the lowest protein concentration for all samples from that particular iteration of the experiment (ranges of 13 to 27 μg). Precast zymogram gelatin and casein gels (Bio-Rad, Inc., Hercules, CA) were loaded and subjected to electrophoresis for 100 min with 125 V at room temperature using Powerpac 1000 (Bio-Rad, Inc., Hercules, CA) according to the manufacturer's specifications. Following electrophoresis, gels were renatured in Novex zymogram renaturing buffer (Invitrogen, Carlsbad, CA) for 30 min at room temperature and then incubated overnight at 37°C in Novex zymogram developing buffer (Invitrogen) to allow degradation of the substrate (gelatin or casein) in the gel matrix. The gels were then washed and stained with 0.4% (wt/vol) Coomassie brilliant blue R-250 (Fisher Scientific, Inc., Fairlawn, NJ) for 1 h then successively destained until distinct bands appeared against a blue background, indicating degradation of the substrate in the gel matrix. Gelatin zymograms are used to detect gelatinase activity, whereas detectable activity on casein zymograms is generally taken to reflect elastase activity. On each gelatin gel, human MMP-9 (trivial names, gelatinase B and type IV collagenase) and MMP-2 (trivial name, gelatinase A), and on each casein gel, human MMP-12 (trivial name, macrophage metalloelastase), were loaded as standards according to the manufacturer's specifications (Chemicon, Inc., Temecula, CA). Semiquantitative analysis of zymogram activity was conducted essentially as previously described (26). Photographs of gels were scanned as described above for transcriptional profiling, and pixel density was analyzed using Scion Image Beta 4.02 software (Scion Corporation, Frederick, MD). Background normalization was conducted for reading from each zymogram.

Western blot analysis. Using the same homogenate samples prepared for zymography as described above, 60 μg of total protein was loaded with (reducing) or without (nonreducing) β-mercaptoethanol and heating onto precast 10% Tris-HCl polyacrylamide-ready gels (Bio-Rad, Inc.). The inclusion of the reducing agent was used to determine the presence of disulfide-linked dimers of MMP-9 versus monomers (45). Precision Plus protein dual-color standards were used to determine the approximate molecular masses of resolved proteins (Bio-Rad, Inc.). Electrophoresis was conducted for 55 min with 200 V at room temperature using a model 200/2.0 power supply (Bio-Rad, Inc.). Separated proteins were transferred to a polyvinylidene difluoride (PVDF) membrane (Bio-Rad, Inc.) for 2 h with 25 V at 4°C using Powerpac 1000 (Bio-Rad Inc). Membranes were blocked overnight at 4°C with a casein blocking buffer. To detect MMP-2 (gelatinase A) protein, PVDF membranes were probed with 0.25 μg/ml polyclonal goat anti-mouse MMP-2 (R&D Systems, Inc., Minneapolis, MN) and binding was detected using a 2×10^{-4} dilution of peroxidase-conjugated rabbit anti-goat immunoglobulin G (IgG; Pierce-Endogen, Rockford, IL). For detection of MMP-9 (gelatinase B) protein, PVDF membranes were probed with 1.5 μg/ml monoclonal anti-mouse MMP-9 (R&D Systems, Inc.) and binding detected with a 3×10^{-4} dilution of peroxidase-conjugated goat anti-rat IgG (Pierce-Endogen). Membranes were developed in Super Signal West Pico substrate (Pierce-Endogen) for 5 min and exposed to Kodak Biomax ML film for 1 h.

EIA for MMP-2 and MMP-9. The same homogenate samples prepared for zymography and Western blotting as described above were used for the antigen capture EIA detection of total MMP-2 and proMMP-9 according to the manufacturer's instructions (R&D Systems, Inc., Minneapolis, MN). Average values were obtained from duplicate samples. When values for a specific sample fell outside of the range of the standards, separate aliquots were thawed, rediluted to achieve a value within the range of the standard curve of the assay, and assessed again. Values were then standardized to protein content and dilution factor (if used) and are reported as ng of total MMP-2 or proMMP-9 per mg of protein for that sample.

Immunohistochemistry for neutrophil-associated MMP-9. At day 14 postinfection, a portion of the mice was euthanized and genital tract tissues were excised and embedded in optimum cutting temperature embedding media (Sakura Finetek, Inc., Torrance, CA). Day 14 was selected because our experience indicated this to be a time of fairly uniform involvement of oviduct with regard to ascension of the infection and accompanying inflammation in this

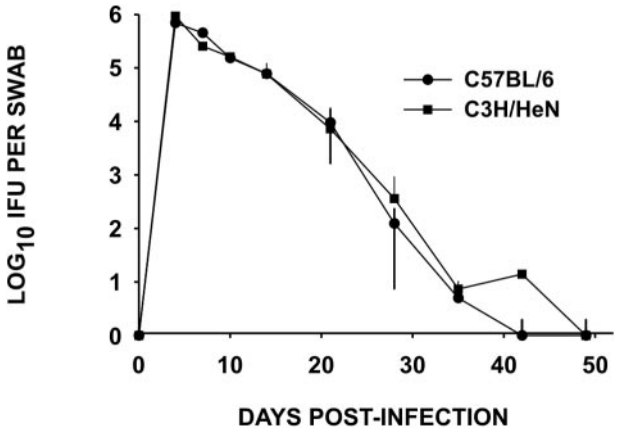

FIG. 1. Course of MoPn urogenital infection in C3H/HeN mice. MoPn was isolated from cervical-vaginal swabs in HeLa 229 monolayers, and the numbers of IFU derived from each swab were counted. Each point in the graph indicates the mean IFU ± (error bars) the standard deviation of 10 mice. No significant differences were observed between the two strains by a two-way analysis of variance (strain, days).

model. Once embedded, the sections were frozen immediately at −25°C and then transferred to −70°C. Serial 4 μM longitudinal sections were cut on a Thermo-Shandon cryotome, and sections were mounted on glass slides fixed in methanol at −20°C for 10 min, rinsed in cold PBS (pH 7.2), and blocked in 5% normal rabbit serum in PBS at room temperature for 20 min. For peripheral blood neutrophils, mice were anesthetized and blood was collected via the retroorbital venous plexus. Peripheral blood neutrophils were isolated by density gradient purification over Ficoll-Hypaque (24) density gradients, and a suspension of the derived neutrophils was adhered to glass slides, fixed with methanol, and blocked in 5% rabbit serum in PBS as described above. Fixed and blocked neutrophil preparations and cryosections of tissues were then incubated with a mixture of the following primary antibodies: (i) a protein-G-purified RB6-8C5 (rat IgG2b anti-granulocyte-specific monoclonal antibody) that was originated by R. L. Coffman, the hybridoma kindly provided to us by Michael Hensel of the Institut fuer Klinische Mikrobiologie, Immunologie und Hygiene, Elangen, Germany) diluted 1:200, and (ii) polyclonal goat anti-mouse MMP-9 (R&D Systems, Inc.) diluted to a 1:100 concentration. The slides were then rinsed and a cocktail of secondary antibodies and 0.1 μg/ml of 4′,6-diamidino-2-phenylindole dihydrochloride (DAPI; Sigma Chemical Company, St. Louis, MO) was made. The secondary antibodies were fluorescein isothiocyanate (FITC)-conjugated rabbit anti-rat IgG (Sigma) at a 1:100 dilution in PBS with 2% normal rabbit serum and tetramethyl rhodamine isothiocyanate (TRITC)-conjugated rabbit anti-goat IgG at a 1:100 dilution in PBS with 2% normal rabbit serum. Following a final rinse in PBS, the slides were then covered with glass coverslips utilizing Aquapolymount (Polysciences, Inc., Warrington, PA) as the mounting medium. Mounted slides were viewed on a Ziess Axiovert 25 fluorescence microscope with a mounted Axiocam MRc5 digital camera and Axiovision 4.2 image-capturing software (Carl Zeiss USA, Inc., Thornwood, NY). Captured images were processed in Corel Draw 11.0 and exported in appropriate file format for publication purposes.

RESULTS

Infection course. The infection course for MoPn urogenital infections in female mice has been described in several studies (34), and our present results did not vary significantly from these prior reports (Fig. 1). This figure is presented for reference purposes only. In general, the infection peaked between 4 and 10 days postinoculation, averaging between 10^5 and 10^6 IFU isolated from the cervical vaginal swabs of each mouse. The infection naturally ascends the upper genital tract rapidly, reaching the oviduct by 7 to 10 days following infection. This ascension of the pathogen to the upper genital tract is followed closely by vigorous acute inflammatory infiltrates in the uterus by 7 to 10 days and the oviduct by 10 to 14 days. The IFU count begins to decline by 10 to 14 days postinfection and resolves between 28 and 35 days postinfection with only an occasional IFU isolated beyond day 35. It should be noted that we have observed the persistence of chlamydial DNA consistently well beyond these time points and in and certain situations, viable organisms can be recovered again following immune suppression (5, 35).

MMP- and TIMP-targeted gene transcriptional profiling in upper genital tract tissue in response to MoPn infection. Table 1 shows the results of mini-gene array analysis targeting the assessment of 18 murine MMP genes and 4 TIMPs. In this table, expression is shown as a numerical increase, a numerical decrease, or no change in transcriptional activity in the specific genes relative to day 0 postinfection for both C3H/HeN and C57BL/6 mice. Due to the likelihood of multiple factors influencing MMP and TIMP gene expression in vivo and the resulting wide variances in RNA abundance at any given point in time in a given mouse tissue, we considered it appropriate to apply a stringent standard for relative changes in gene expression. Hence, we arbitrarily considered a relative increase in expression as ≥1.5-fold (≥50%) whereas a decrease in expression was considered ≤0.5 (≤50%). Thus, a change by a factor of 0.5 to 1.5 (50% decrease to 50% increase) was considered no change and is shown as such in Table 1. Were the same assessments conducted under strictly controlled in vitro conditions, one could consider smaller variances in expression significant.

In general, it was observed that C3H/HeN mice expressed more MMP transcriptional activity than the C57BL/6 mice through day 21 postinfection. Particularly enhanced in this strain through day 21 in response to the infection were the genes for MMP-13 (trivial name, collagenase 3), which degrades interstitial or fibrillar collagens; MMP-10 (trivial name, stromelysin 2); MMP-15; MMP-17 (trivial name, membrane type 4 MMP, or MT4-MMP); MMP-3 (trivial name, stromelysin 1); MMP-9 (trivial name, gelatinase B or type IV collagenase); MMP-12 (trivial name, macrophage metalloelastase); and that of its natural tissue inhibitor, TIMP-1. Other genes were observed to be either intermittently increased in expression (e.g., collagenase A, MMP-20) or relatively unchanged by our criteria. Particularly consistent expression throughout the experiment was observed for MMP-2. The sole gene that appeared to be decreased in response to infection in C3H/HeN mice was MMP-7 (trivial name, matrilysin), which is largely an epithelial-cell-derived MMP. Thus, this decrease could be a result of extensive epithelial damage occurring during the infection and the resulting loss of a primary source of this MMP.

Interestingly, in C57BL/6 mice, the expression of most of the assessed genes remained unchanged relative to day 0 and, when changes were noted, decreases in expression were often seen. Beyond day 21 in both strains, MMP and TIMP genes tended to display decreased expression, with the exception of day 35 in the C3H/HeN strain and the TIMP-1 gene at day 56 in the C3H/HeN strain, which were somewhat elevated. The activity of TIMP-2, TIMP-3, TIMP-4, or MMP-2 genes was relatively unchanged in either mouse strain throughout the course of the experiment.

TABLE 1. Transcriptional analysis of MMP and TIMP genes

Gene	Mean expression on indicated day postinfection[a]															
	4		7		10		14		21		28		35		56	
	C57	C3H	C57	C3H	C57	C3H	C57	C3H	C57	C3H	C57	C3H	C57	C3H	C57	C3H
Collagenase-A	NC	NC	0.5	NC	NC	2.9	NC	NC	NC	2.1	NC	0.1	0.2	NC	0.4	NC
MMP-10	NC	1.6	NC	2.1	NC	3.0	NC	1.8	NC	2.5	0.5	0.5	0.5	1.5	0.1	0.2
MMP-11	NC	NC	NC	NC	NC	2.1	NC	NC	NC	NC	NC	NC	0.5	2.1	NC	0.3
MMP-12	NC	2.2	0.5	2.0	NC	2.6	0.4	NC	0.2	3.9[b]	0.3	0.3	0.3	1.8	0.4	NC
MMP-13	NC	13.9[b]	NC	28.6[b]	NC	23.5[b]	NC	15.4[b]	0.5	30.3[b]	NC	NC	NC	3.5	0.3	NC
MMP-14	NC	NC	NC	NC	NC	NC	NC	NC	NC	NC	0.5	NC	NC	NC	NC	NC
MMP-15	NC	3.5	NC	NC	NC	3.2	NC	1.9	0.4	5.5[b]	0.4	NC	0.3	2.6	0.3	1.6[b]
MMP-16	NC	NC	NC	NC	NC	NC	NC	NC	0.5	NC	NC	NC	NC	NC	0.5	NC
MMP-17	NC	2.0	NC	2.0	NC	NC	NC	1.8	NC	1.5	0.5	0.3	0.5	2.0	0.1[b]	NC
MMP-19	NC	NC	NC	NC	NC	NC	NC	NC	NC	1.5	0.5	NC	0.5	NC	NC	NC
MMP-2	NC	NC	NC	NC	NC	NC	NC	NC	NC	NC	NC	NC	NC	NC	0.5	NC
MMP-20	NC	2.3	NC	2.2	NC	NC	NC	NC	NC	2.1	NC	NC	0.4	2.0	0.3	NC
MMP-23	NC	NC	NC	NC	NC	NC	NC	NC	0.5	NC	0.2	0.3	0.4	NC	0.4	NC
MMP-24	NC	1.8	NC	NC	NC	NC	NC	NC	NC	NC	0.2	NC	0.4	NC	0.3	0.5
MMP-3	NC	1.8	1.8	3.3	NC	1.9	NC	NC	NC	1.8	NC	NC	NC	NC	0.3	NC
MMP-7	NC	NC	NC	0.4	NC	NC	NC	0.3	NC	NC	0.4	0.4	NC	NC	0.4[b]	0.2
MMP-8	NC	3.6	NC	1.5	NC	NC	NC	NC	NC	NC	NC	NC	NC	NC	0.5	0.3
MMP-9	NC	4.1[b]	NC	4.3[b]	NC	3.0	NC	1.8	2.2	3.0	NC	NC	NC	1.6	0.5	NC
TIMP-1	NC	NC	1.5	3.0	NC	2.4	0.5	2.2	NC	2.0	0.2	NC	NC	NC	NC	2.2
TIMP-2	NC	NC	NC	NC	NC	NC	NC	NC	NC	NC	NC	NC	NC	NC	NC	NC
TIMP-3	NC	NC	NC	NC	NC	NC	NC	NC	NC	NC	NC	NC	NC	NC	NC	NC
TIMP-4	NC	NC	NC	NC	NC	NC	NC	NC	NC	NC	NC	0.3	NC	NC	NC	NC

[a] Values are the mean of four to six mice per time point in two or three different experiments (depending on the time point) and are expressed relative to P4 pretreatment from day 0 (uninfected), where 1.0 equals day 0 values. We arbitrarily considered a relative increase in expression as ≥1.5 (50% or more above day 0), whereas a decrease in expression was considered ≤0.5 (50% or more below day 0). Hence, a 0.5 to 1.5 (50% decrease to 50% increase) expression value relative to day 0 was considered no change (NC).

[b] Significant difference between mouse strains at the specified time point was observed using a two-sided *t* test. *P* values varied but in each case were <0.5.

Assessment of MMP activity by zymography. Gelatin and casein zymography are useful tools in assessing the activity of gelatinases and elastases, respectively, in various biological samples. They allow qualitative and semiquantitative assessment of the activity of both the zymogen and activated forms of the enzymes against the targeted substrates.

Figure 2A and B shows the activity of a lower-molecular-mass gelatinase, in upper urogenital tract homogenates from infected C3H/HeN and C57BL/6 mice at the specified time points following infection. Panel A shows that this gelatinase activity comigrated with human zymogen MMP-2 standards—a 72-kDa latent and 68-kDa active form on gelatin zymography. The identity of this activity as MMP-2 was confirmed by Western blotting, which mirrored its constitutive expression by zymography (data not shown). The persistent presence of MMP-2 in either its zymogen or more active form is consistent with the stable MMP-2 gene expression observed and described above and in Table 1. We also confirmed consistent MMP-2 gene transcription throughout the infection course by reverse transcriptase PCR and Western blotting (data not shown) and by antigen capture EIA (see Fig. 5, below). A summary of total MMP-2 activity and semiquantitative assessment of the enzyme's activity as assessed on zymography is shown in the top of Fig. 2B. Total zymogram (higher-molecular-mass latent and lower-molecular-mass active form) activity was assessed and is shown in this figure. While zymograms indicated an overall trend toward enhanced MMP-2 expression and zymograph activity following infection, this was not found to be significant with the exception of a significant spike in gelatinolytic activity on day 7 for the C3H/HeN mice (Fig. 2B, top). This activity was also significantly elevated relative to the C57BL/6 strain. A significant difference in MMP-2 activity on day 28 was also observed between the two strains but was not significantly elevated relative to day 0 in either strain. However, a similar difference was observed at day 14 in the uninfected mice and was attributable to high MMP-2 activity in homogenates from two of six C3H/HeN mice at that time (Fig. 2B, bottom). Hence, while some variances occurred, we could not conclude that any of these were specifically attributable to a response to infection.

A separate higher-molecular-mass gelatinolytic activity in tissue homogenates derived from infected mice was observed. The gelatin-clearing bands indicating this activity migrated to between 100 and 110 kDa. The recombinant human MMP-9 used for a standard in these zymograms migrated at the expected 92 kDa (Fig. 3A). We ascribed this activity to MMP-9 due to its proximity to human MMP-9; its apparent molecular mass in zymograms corresponded to murine MMP-9, which has been estimated at 105 to 110 kDa (25, 41), and the presence of a comigrating MMP-9-specific signal on a mouse-specific MMP-9 Western blot (see Fig. 4, below). In three to four separate experiments and a total of six to eight mice assessed at each time point, the increase in MMP-9 activity was observed only in tissue homogenates of mice which were infected with MoPn. Mice that were pretreated with P4 but not infected and run in parallel with infected mice only occasionally showed MMP-9 activity, and this was observed at very low levels.

A summary of total monomer MMP-9 activity and semiquantitative assessment of the enzyme's activity as assessed on zymography throughout the 56-day monitoring period is shown

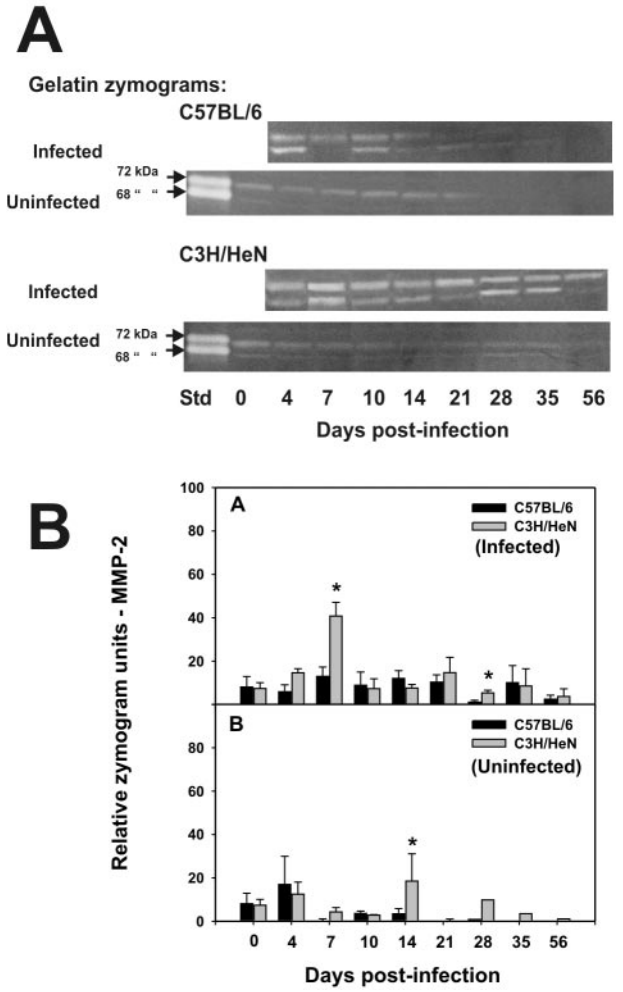

FIG. 2. Gelatin zymography for total MMP-2. Panel A shows typical zymograms of homogenized upper genital tract tissues from infected and uninfected C57BL/6 (top) and C3H/HeN (bottom) mice at various days postinfection. Both the 72-kDa latent and 68-kDa active forms have gelatinolytic activity on zymography (arrows, first lane in zymograms with uninfected mice). Abbreviations: Std, recombinant human MMP-2 standards. Panel B shows the results of gelatin zymography relative to total MMP-2 in upper genital tract homogenates. The top half of panel B represents the composite zymography results for infected mice, whereas the bottom half of panel B represents the same for uninfected controls followed in parallel with the infected mice. The black and gray bars represent the mean total MMP-2 gelatinolytic activity for tissues derived from C57BL/6 and C3H/HeN mice, respectively (six to eight samples per time point; results are composites of three or four experiments), plus or minus the standard deviation of the mean for each (error bars). Other than days 7 ($P < 0.01$, two-way t test) and 28 ($P < 0.04$, two-way t test) for infected C3H/HeN mice and day 14 ($P < 0.02$, two-way t test) for uninfected C3H/HeN mice, there was no significant elevation in MMP-2 activity relative to the C57BL/6 strain or to the uninfected mice in either strain. Asterisks indicate significant differences between strains of mice.

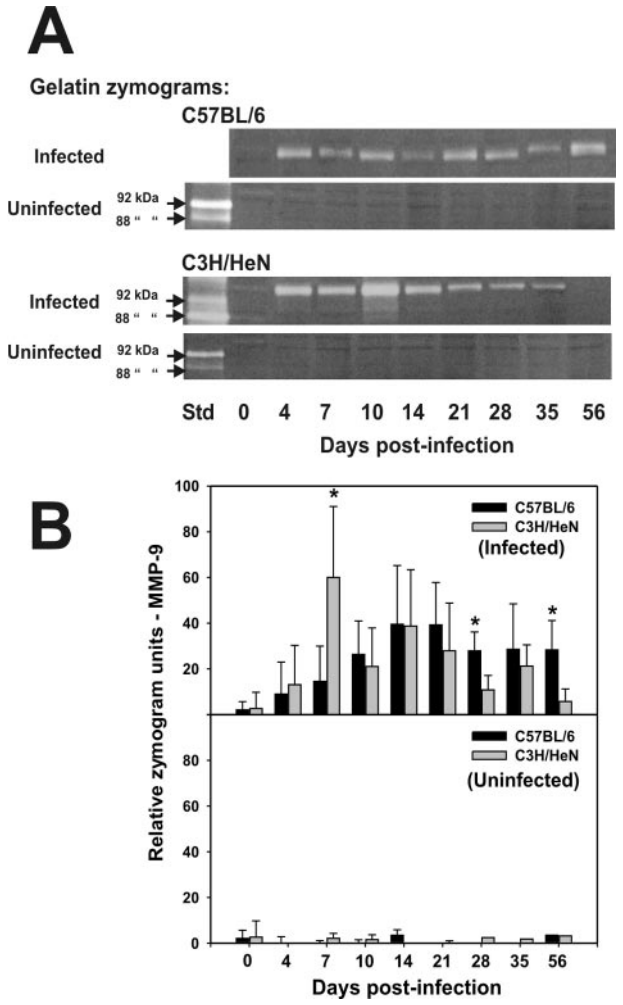

FIG. 3. Gelatin zymography for monomeric MMP-9. Panel A shows representative zymograms of homogenized upper genital tract tissues from infected and uninfected C57BL/6 (top) and C3H/HeN (bottom) mice at various days postinfection. Both the 92-kDa latent and 88-kDa active forms have gelatinolytic activity on zymography (as labeled with arrows). The approximate predicted molecular mass of murine monomer MMP-9 at 105 kDa is also labeled (arrows). Abbreviations: Std, recombinant human MMP-9 standards. Panel B shows the results of gelatin zymography relative to total monomer MMP-9 in upper genital tract homogenates. The top half of panel B represents the composite zymography results for infected mice, whereas the bottom half of panel B represents the same for uninfected controls followed in parallel with the infected mice. The black and gray bars represent the mean monomer MMP-9 gelatinolytic activity for tissues derived from C57BL/6 and C3H/HeN mice, respectively (six to eight samples per time point; results are composites of three or four experiments), plus or minus the standard deviation for each (error bars) Gelatinolytic activity was significantly elevated in samples derived from infected C3H/HeN mice relative to day 0 and to samples derived from uninfected C3H/HeN mice beginning day 7 postinfection through day 21 and also day 35 (P values varied but were <0.04 by a two-way t test in each case). In C57BL/6 mice, monomer MMP-9 gelatinolytic activity was elevated relative to day 0 beginning on day 7 and remained significantly elevated through day 56 ($P < 0.05$ in each case). Asterisks indicated significant differences observed between strains at days 7 ($P < 0.01$), 28, and 56 ($P < 0.04$ for each).

in the upper section of Fig. 3B. Monomer MMP-9 activity was reported only for MMP-9, although a thin band of gelatinolytic activity could sometimes be discerned migrating at the anticipated molecular mass of the dimer form of MMP-9 (data not shown). The lower section of Fig. 3B represents the cumulative

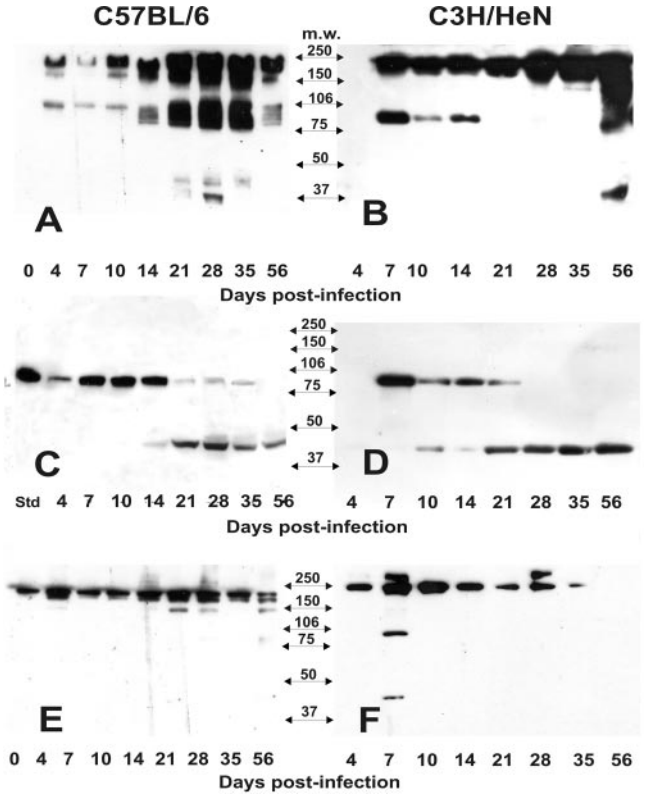

FIG. 4. Western blot detection of MMP-9 activity. Panels A and B represent the results of Western blots of nonreducing gels of upper genital tract tissue homogenates derived from infected C57BL/6 and C3H/HeN mice, respectively. Panels C and D represent the results of Western blots of reducing gels of the same samples in panels A and B with the exception of the first lane in panel C, which was loaded with recombinant murine MMP-9 (Std, standard). Panels E and F represent Western blots of nonreducing gels of upper genital tract homogenates derived from uninfected C57BL/6 and C3H/HeN mice, respectively. No MMP-9 signal could be detected in Western blot gels of reduced samples derived from uninfected mice (data not shown). Arrows between the panels are labeled to represent the approximate electrophoretic migration of commercially prepared molecular mass markers in each gel.

data for zymograms of the upper urogenital tissue from uninfected mice.

A consistent observation noted was that the increased MMP-9 activity was detected earlier in C3H/HeN mice (six of eight at day 4 and eight of eight at day 7) than in C57BL/6 mice (two of eight at day 4 and four of eight at day 7). The difference between the strains was significant at day 7, with C3H/HeN sustaining a higher activity than the C57BL/6 mice ($P < 0.01$ by a two-way t test). However, C57BL/6 mice possessed higher MMP-9 activity on zymograms of samples obtained at days 28 and 56 postinfection ($P < 0.04$). The activity for C57BL/6 samples remained significantly elevated relative to day 0 from day 7 through day 56 postinfection and for C3H/HeN mice for day 7 through day 21 and also day 35. It should be noted that uninfected mice had no significant increase in MMP-9 activity on zymograms at any time postinfection. In mice that were not pretreated with P4 and not infected, some background MMP-9 activity could be detected but was significantly elevated in response to the infection in a manner similar to that of P4-pretreated mice (data not shown). Thus, while P4 tended to suppress MMP-9 activity on zymograms of tissue homogenates derived from uninfected mice, the overall activity observed following infection was no different than that for mice not treated with P4.

On casein zymography, two bands were inconsistently observed in urogenital tissue homogenate samples following infection in both C3H/HeN and C57BL/6 mice. The first was a higher-molecular-mass band, indicating casein degradation, that comigrated with the recombinant human MMP-12, standard at ca. 57 kDa and probably representing the murine homolog of this enzyme. A low-molecular-mass band was also seen. This was mostly observed in uninfected mice and even enhanced up to 14 days postinfection in these controls that were run in parallel. We believe this latter casein-degrading activity to be attributable to an epithelial metalloproteinase, MMP-7 which can have elastolytic activity (19). Also, unlike other MMPs, MMP-7 does not contain a hemopexin domain and is therefore of considerably lower molecular mass than other members of the MMP family (49). Its latent form is 28 kDa, whereas an intermediate and a fully active form migrate at ca. 21 and 19 kDa, respectively. The observed lower-molecular-mass casein-degrading band migrated at less than 20 kDa. MMP-7 is produced primarily by epithelial cells, and this would explain its enhancement in uninfected mice on casein zymograms because progesterone is known to maintain and enhance the epithelial lining in the female upper genital tract. A decrease in gene expression for MMP-7 during peak infection in the infected mice, as seen in Table 1, is likely attributable to the considerable damage to the urogenital epithelium that routinely occurs, particularly in the susceptible C3H/HeN strain. Unfortunately, we have found that casein zymograms do not stain with sufficient resolution to clearly photograph or assess for semiquantitative analysis, as was described above for gelatin zymograms. At the time of these experiments, commercial polyclonal or monoclonal antibodies against murine MMP-7 were not available for further confirmation of this activity by Western blotting.

Western blot assessment of MMP-2 and MMP-9 expression. In order to verify that the observed gelatinolytic activity on zymography was attributable to MMP-2 and MMP-9, we used Western blotting of proteins resolved under both reducing and nonreducing conditions. The samples used were parallel aliquots of the samples used in the zymography described above.

As we anticipated, Western blotting confirmed the presence of MMP-2 in all samples, regardless of infection, with some sporadic fluctuation in levels that did not necessarily correlate with infection (data not shown). A high-molecular-mass (approximately 250 kDa) signal was seen on Western blots of sodium dodecyl sulfate-polyacrylamide electrophoresis gels of samples under nonreducing conditions that was not seen on Western blots of the same samples under reducing conditions. We interpreted this result as indicating a multimeric complex of latent MMP-2 or MMP-2 with TIMP-1 and MMP-14 (also known as membrane type metalloproteinase 1, or MT1-MMP), as has been reported for the human form of the molecule (22). For samples treated under reducing conditions, bands at 72 kDa and several lower-molecular-mass bands ranging from ca. 47 to 67 kDa could be observed at times. The former likely represented proMMP-2 enzyme and the latter represented

more active cleavage products of the same. Western blots of tissue homogenate samples derived from uninfected mice showed a banding pattern similar to that of the infected mice, whereas reducing conditions abrogated this pattern in both infected and uninfected mice. Hence, we concluded that MMP-2 was not significantly up-regulated in response to infection and this roughly correlates with our findings on gelatin zymography in Fig. 2A.

Figure 4 shows results for Western blot detection of MMP-9 in homogenates of upper genital tracts from infected and uninfected mice. Panels A and B show the results of homogenates of the upper genital tract tissue from infected mice over time under nonreducing conditions, whereas panels C and D are identical samples run under reducing conditions. Panels E and F represent Western blots of samples derived from uninfected mice run in parallel with infected ones under nonreducing conditions. Only results for nonreducing conditions are shown for samples from uninfected mice due to a lack of detection of any signal from Western blots of gels of tissue homogenates from these mice that were run under reducing conditions. This observation is likely due to a fivefold reduced sensitivity of the detecting antibody under reducing conditions (specified in the manufacturer's product information).

In samples derived from uninfected but P4-pretreated mice run in parallel with infected mice, we could often detect a high-molecular-mass signal that migrated just below the 250-kDa molecular mass marker (Fig. 4E, day 0). We believe this to be the homodimeric form of MMP-9 (ca. 220 kDa). Progesterone pretreatment tended to suppress this signal but only briefly, and this observation was consistent with the zymography results described above. In Fig. 3A and B, which represents nonreducing conditions for samples derived from infected mice, we observed increased expression of the high-molecular-mass dimeric MMP-9 signal in response to infection in both the C57BL/6 and C3H/HeN strains of mice. This increase was noted as early as day 4 (C57BL/6) and was particularly prominent at day 7 postinfection in the C3H/HeN mice. It appeared to be substantially elevated in both strains beyond day 10 and throughout the remaining 56-day monitoring period.

In the same figure in panels A and B compared to panels E and F, we observed what appeared to be the expression of monomeric MMP-9 at ca. 100 to 105 kDa. This band appeared beginning on days 4 and 7 in the C57BL/6 and C3H/HeN mice, respectively. However, there were distinct differences between mouse strains in the expression of monomeric MMP-9 that began as early as day 4 postinfection (Fig. 3B and D). C3H/HeN mice expressed relatively high levels of MMP-9 monomer from day 7 through day 14, but this band could not be detected beyond day 14 in this strain of mice. C57BL/6 mice also expressed MMP-9 monomer through day 14 but at lower levels than the C3H/HeN mice (Fig. 3A and C). Beginning about 14 days postinfection and beyond, C57BL/6 expressed high levels of MMP-9 monomer forms through day 35—a time point when the monomer cannot be detected in the C3H/HeN mice. In C57BL/6 mice, the monomer band actually appeared at four distinct molecular mass bands migrating just below the 106-kDa marker on days 14 and 56 postinfection, with a stronger blurred signal at the same molecular mass range at days 21 to 56.

Another interesting result was observed when Western blots of sodium dodecyl sulfate-polyacrylamide electrophoresis gels were run under reducing conditions (Fig. 4C and D). As expected, the signal associated with dimeric MMP-9 seen in panels A and B was completely abrogated but the signal associated with the MMP-9 monomer was retained. However, an additional band in the ca. 42- to 45-kDa range was observed between days 10 (C3H/HeN) and 14 (C57BL/6) postinfection and persisted through day 56 with a concurrent reduction of the higher-molecular-mass MMP-9 band signal strength. Because the detecting antibody in this assay is monoclonal and specific for proMMP-9, it is likely that this represents the further post-translational processing of MMP-9 and possibly further conversion to a more inactive form of the molecule by degradation with other MMP, as has been reported for MMP-3 and MMP-13 (14, 45). Nearly all detectable MMP-9-specific signals in reduced samples from C3H/HeN mice beyond day 21 were of this form. As previously mentioned, it should be noted that this detecting antibody loses sensitivity under reducing conditions and this may account for the loss in signal strength. Finally, we were unable to detect any signal on Western blots of samples subjected to reducing conditions from uninfected mice (same samples in Fig. 4E and F) and this too was likely attributable to a loss in sensitivity of the assay under reducing conditions (data not shown).

EIA for MMP-2 and MMP-9. In order to further confirm the production of MMP-2 and MMP-9, we used commercially available antigen capture EIAs. When referencing these data, it is important to note that the assay for MMP-2 measures total MMP-2 (both active and latent forms) whereas that for MMP-9 measures only proMMP-9 (only latent forms) of the molecules.

In Fig. 5A, we found no significant change in total MMP-2 compared to preinfection levels in either strain of mice. However, total MMP-2 was elevated at days 0, 21, and 28 postinfection in the C3H/HeN mice when compared to the C57BL/6 mice by a two-tailed unpaired *t* test ($P < 0.008$ and $P < 0.04$, respectively).

Both strains of mice displayed significantly elevated levels of proMMP-9 following infection (Fig. 5B). For the C57BL/6 strain, a response was evident in some mice as early as day 4 (four of six responding above day 0 levels; range of responders; 5.5 to 56.6 ng/ml; $P < 0.04$ by two-tailed unpaired *t* test). For the C3H/HeN mice, this difference was first observed and also peaked on day 7 postinfection (seven of seven responding above day 0 levels; range, 6.5 to 114 ng/ml; $P < 0.02$). The proMMP-9 remained elevated in both strains relative to day 0 throughout the remainder of the 56-day monitoring period. Though a trend toward higher proMMP-9 production was observed in the C57BL/6 mice when compared to the C3H/HeN strain, wide variances between mice on any given time point prevented these from obtaining significance with the exception of 21 days postinfection ($P < 0.02$). Considering that this assay detects proMMP9, these data correlate with the loss of monomer and the appearance of the <50-kDa band in Fig. 4C and D.

Evidence that neutrophils are a significant source of presynthesized MMP-9 during MoPn urogenital infection. Because we observed significantly enhanced MMP-9 protein levels (by EIA and Western blot analysis) and activity (by gelatin zymography) at time points postinfection correlating with peak in-

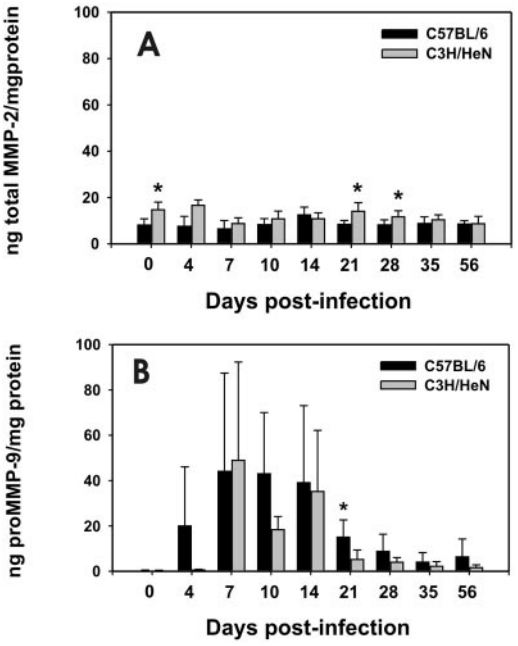

FIG. 5. Detection of total MMP-2 and proMMP-9 by antigen capture EIA. (A) These data represent the mean nanograms (ng) of total MMP-2 per mg protein in upper urogenital tissue homogenates derived from C57BL/6 (black bars) or C3H/HeN (gray bars) mice plus or minus the standard deviation (error bars). There was no significant elevation in total MMP-2 by this assay in either strain at any time point postinfection relative to day 0. However, total MMP-2 was elevated in C3H/HeN relative to C57BL/6 mice on days 0, 21, and 28 postinfection ($P < 0.04$ in each case by a two-way t test). (B) These data represent the ng of proMMP-9 per mg total protein in the same upper genital tract homogenates shown for total MMP-2 in panel A. Significant elevation in proMMP-9 relative to day 0 was first observed in C57BL/6 mice at day 4 and for C3H/HeN mice at day 7 and persisted through day 56 for both strains ($P < 0.05$ by a two-way t test in each case). A significant elevation of proMMP-9 in the C57BL/6 mice relative to the C3H/HeN mice was observed on day 21 postinfection ($P < 0.02$).

flammatory responses, we sought to determine which leukocyte populations infiltrating the affected tissue could be producing it. Thus, we hypothesized that neutrophils could be a significant source.

Figure 6 shows immunohistochemistry results on a C3H/HeN mouse oviduct at day 14 postinfection. Day 14 was selected because our results indicated that a maximal amount of MMP-9 production and activity was evident during this time frame (see above) and because day 14 corresponds to peak acute neutrophilic inflammatory responses on hematoxylin and eosin-stained sections as well as significant pyosalpinx by macroscopic observation (39). Panel A is a photomicrograph of specific fluorescence on the FITC wavelength filter (green) and indicates staining with monoclonal antibody RB6-8C5, a granulocyte-specific monoclonal antibody (16). Nuclei were labeled with DAPI and stained blue. As can be seen in this panel, an intense polymorphonuclear granulocyte infiltrate is observed throughout the stromal layers and lamina propria and exuding into the lumen of the oviduct, which is filled with similarly stained cells. Fig. 6B is a photomicrograph of the same section but with the TRITC wavelength filter (red) utilized and indicates specific staining with monoclonal antibody directed against murine MMP-9. The cellular staining pattern is identical to that observed in panel A with the exception that considerable diffuse staining is observed near the lamina propria at the basolateral aspect of the oviduct epithelium and also within the lumen of the oviduct (Fig. 6B, arrows). This diffuse extracellular staining is less intense or altogether absent as one proceeds away from the oviduct lumen and lamina propria where MMP-9-specific staining is found almost entirely intracellular within the granulocyte infiltrate. We attribute this diffuse staining pattern to MMP-9 release at the site just prior to or during transepithelial migration into the lumen. Interestingly, type IV collagen, a primary constituent of the epithelial basal lamina, is a ready substrate for MMP-9. Panel C is an overlay of panels A and B. The yellow staining pattern indicates colocalization of granulocyte and MMP-9-specific staining patterns such that nearly all MMP-9 cellular staining is associated with infiltrating granulocytes. Given that previous results have shown that >95% of the granulocytes present in this time frame are neutrophils and only a small minority of other granulocytes (e.g., eosinophils) (7, 39, 40), we interpret these results to indicate that at least one source of MMP-9 is the primary acute inflammatory cell in this model: the neutrophil. Panel D is a preparation of peripheral blood neutrophils from a normal, uninfected mouse stained in an identical fashion as for the cryosection in panel B. Note that there is intense cytoplasmic staining for MMP-9 in peripheral blood neutrophils. This confirms that murine neutrophils, like their human counterparts, presynthesize MMP-9 and store it in their cytoplasms prior to entry into sites of infection or inflammation (30). Thus, it is not necessary for MMP gene transcription to occur at the site of inflammation. Though the observations depicted in Fig. 6 are from a C3H/HeN mouse, similar results were observed for C57BL/6 mice with differences not detectable between the two strains. The lack of differences between the two strains may be attributable to a lack of quantitative sensitivity of immunohistochemistry.

DISCUSSION

In chronic chlamydial diseases of humans such as trachoma and tubal factor infertility, it is generally considered that chronic inflammation is responsible for most sequelae (reviewed in reference 50). However, in the murine model, the degree of antecedent acute inflammation has been linked to chronic chlamydial disease (e.g., hydrosalpinx and infertility [7, 9, 39]). That the acute inflammatory response in many inflammatory or infectious diseases can cause irreversible tissue destruction is not a novel concept (51). Certainly in any situation, the acute inflammatory state should normally represent a coincident but transient modification of the ECM involving MMP and other proteolytic enzymes that allows for the influx of inflammatory cells and the activation of latent host factors. Eventually, this initial response should give way to remodeling and tissue regeneration with restoration to normal function of the affected tissue or organ. Matrix metalloproteinases have a critical role in many physiological processes, including normal tissue repair responses following inflammatory damage (49). However, it has been shown that in many inflammation-related diseases, persisting or excessive inflammation can lead to the excessive expression of MMP, which can result in protracted or

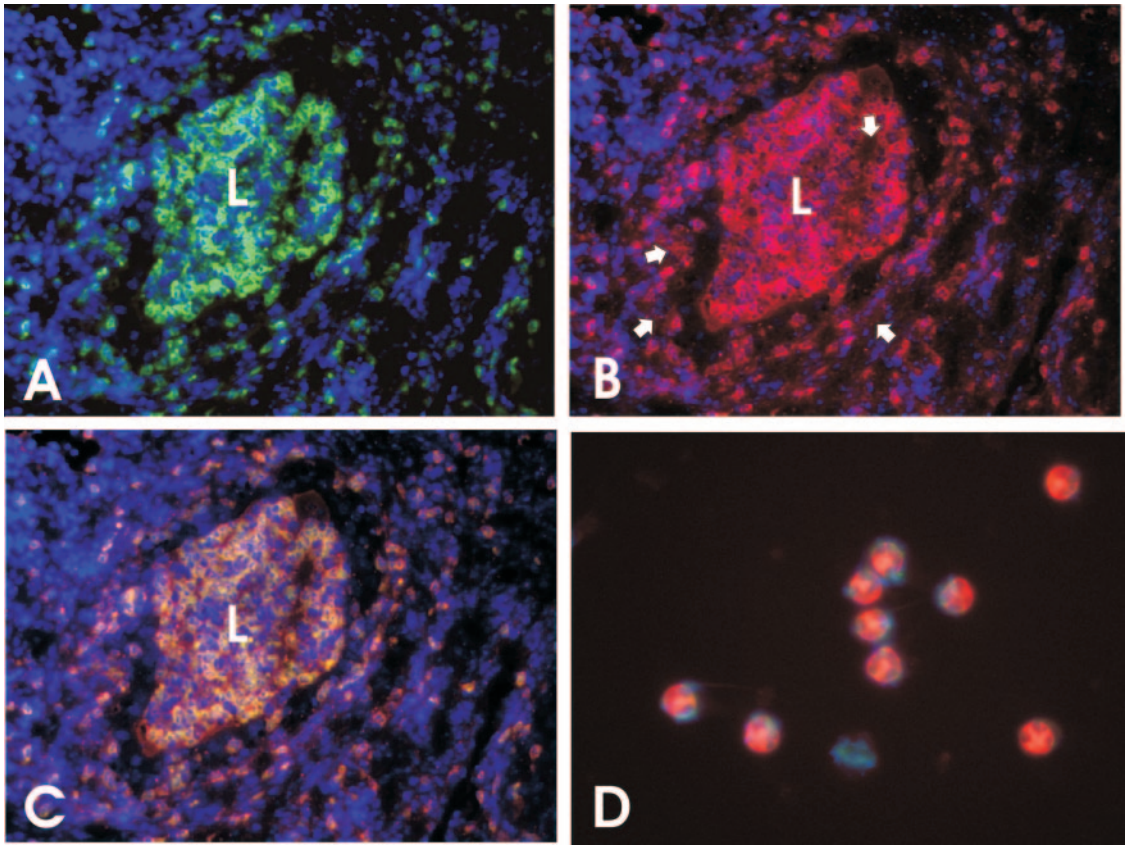

FIG. 6. Immunohistochemical detection of granulocyte-associated MMP-9 in the oviduct of MoPn-infected mice. For panels A through C, cryosections of oviducts taken from a C3H/HeN mouse at day 14 postinfection were triple labeled with monoclonal antibodies against murine granulocytes (FITC-conjugated secondary antibody, green fluorescence), murine MMP-9 (TRITC-conjugated secondary antibody, red fluorescence), and DAPI (nuclear stain for contrast, blue fluorescence). L, oviduct lumen. (A) The section was photographed using a FITC-specific filter. Green fluorescence indicates specific staining for infiltrating polymorphonuclear granulocytes, mostly neutrophils. The staining pattern is mostly cell associated. (B) The same section as viewed and photographed in panel A was then viewed and photographed using a TRITC-specific filter. Red fluorescence indicates MMP-9-specific staining which is mostly cytoplasmic in the same cells that stain with the granulocyte-specific monoclonal antibody shown in panel A. However, near the basal lamina of the epithelium and in the oviduct lumen, diffuse extracellular staining is also seen (white arrows). (C) This is an overlay of the two photographs depicted in panels A and B. Yellow staining indicates colocalization of MMP-9 and granulocyte-specific labeling. (D) This is a purified preparation of peripheral blood neutrophils derived from an uninfected C3H/HeN mouse and stained in an identical fashion as the cryosection shown in panel B. The cytoplasm of peripheral blood neutrophils stains intensely red for MMP-9. Photos were taken using a digital camera as described in the Materials and Methods section. Digitally captured images were processed in Corel Draw 11.0 and exported in appropriate file format for publication purposes.

enhanced repair responses and thus excessive ECM accumulation and fibrosis (reviewed in references 37 and 38). In this regard, we have recently proved that there is extensive ECM modification as a consequence of infection in the murine model of chlamydial urogenital infection (39). It was demonstrated that extensive subepithelial as well as lumen-occluding fibrosis occurs as routine sequelae of MoPn infection in mice and is correlated with hydrosalpinx formation and infertility. These findings, as well as observations of MMP expression in trachoma (1) and the in vitro expression of MMP in response to *C. trachomatis* infection in human fallopian tube organ culture (3), led us to postulate MMP expression in vivo in the murine model.

In the present study, we sought to first explore the expression of several known MMPs in mouse strains characterized as susceptible and resistant depending on rates of hydrosalpinx and infertility subsequent to infection. This study was first conducted on a transcriptional level utilizing commercially available mini-gene arrays targeting known MMP and TIMP genes. To summarize our results, we observed the increased expression of genes encoding several MMPs subsequent to infection in the susceptible C3H/HeN strain of mice. With some exceptions, a similar degree of enhanced MMP expression was not observed in the resistant C57BL/6 strain of mice. For example, the expression of genes for MMP-13 and MMP-9 appeared to be consistently enhanced in the C3H/HeN strain over that of the C57BL/6 strain. Others such as MMP-10 and MMP-12 also appeared to be selectively up-regulated in the C3H/HeN mice over that of the C57BL/6 mice, albeit to a lesser degree. Still other genes, such as those for MMP-3, MMP-8, and MMP-17, were more variable but also trended toward a higher expression in the C3H/HeN mice. Some enhancement in the expression of TIMP-1, which is the natural inhibitor for MMP-9, was also observed at several time points in the C3H/HeN strain, with the expression of the remaining TIMP genes not significantly changed in response to the infec-

tion in either strain. Similarly, the gene for MMP-2 was constitutively expressed and its enzymatic activity on zymography and total MMP-2 protein levels remained relatively constant, as measured by any assay used in this study. This is not an unusual finding for MMP-2, the levels of which are not always changed in response to inflammation but whose absolute activity may be altered through interaction with other MMP. When the latter occurs, it has been reported that MMP-2 can influence the activation of other MMPs (42) and the activity of proinflammatory cytokines (20) in a cascade of enzymatic activation. Because we found that MMP-2 was unaltered in its expression and there was a lack of consistent enhancement in its activity by zymography as a result of infection, we interpret our results to mean that it is unlikely to be involved directly in the pathogenesis of MoPn infection in this model.

The interpretation of these results can be complex due to the fact that MMPs have been shown to be regulated on many levels. This includes transcriptional and translational regulation, post-translational modification, and numerous factors in the extracellular milieu such as free radicals, TIMPs, and other proteases and inhibitors (45, 47, 49, 52). For example, as mentioned previously, neutrophils may presynthesize MMPs (e.g., MMP-9, neutrophil elastase) and release them following cellular activation whereas other cell types produce them constitutively and still others produce them on demand. Our present data confirm these previous observations in that we found that murine neutrophils presynthesize MMP-9 prior to entering the site of chlamydial infection and apparently release the presynthesized MMP-9 upon stimulation at the site (Fig. 6). Hence, transcription of a specific MMP gene does not necessarily correlate with production or activity of the enzyme and, conversely, lack of transcription may not mean the absence of enzyme activity. Thus, the significance of the observed transcriptional differences in the present study lies mostly in the ability to provide a platform of selection and further exploration of specific MMPs and TIMPs and the role they may play in the functional balance of tissue degradation in response to this infection. Though significant progress through this type of work can be accomplished in vivo through the administration of MMP inhibitors and application of various knockout mice, an in vitro system that replicates the interaction of the various players seen in vivo (e.g., epithelial cells, neutrophils, etc.) and allows delineation of the specific regulators involved in MMP release and activation would greatly assist in this process. Some very useful systems have been developed for the study of the transepithelial migration of human neutrophils, though this system has yet to be used for the study of MMPs (13, 54). An analogous murine system is currently being developed in our laboratory to study the interactions between epithelial cells and neutrophils.

A good example of the complexity of the MMP/TIMP system is the production and activation of MMP-9. Whether MMP-9 is immediately available for action on its substrates (largely, type IV collagen of the basal lamina) depends on the type of cell releasing it and the local milieu at the time of its release. As mentioned previously, while MMP-9 can be synthesized by many cell types, in human neutrophils and band cells, it is synthesized prior to exiting the bone marrow and stored in cytoplasmic granules (30). On activation, the neutrophil discharges MMP-9 mostly as a monomer but also as a homodimer or a heterodimer with neutrophil-gelatinase-B-associated lipocalin (NGAL) (30, 45). When derived from neutrophils, each of the forms of MMP-9 is produced sans TIMP-1, which is its normal inhibitor. In contrast, monocyte/macrophage cells transcribe the gene for MMP-9 only when appropriately stimulated and subsequently release the latent form of the molecule. Although MMP-9 derived from macrophages and other cellular sources is released as homodimers without the neutrophil-gelatinase-B-associated lipocalin heterodimer, it is released in a complex with TIMP-1 and thus needs further processing to become fully active (30).

One of the difficulties in working with MMP/TIMP data in a murine system is that many of the reagents available are specific for the human molecules and thus most of the background data available are related to human but not murine MMP and TIMP. Assuming that what is know of human-neutrophil-associated MMP-9 holds true in murine neutrophils, one could interpret our present results to mean that neutrophils are a major source for MMP-9 during acute inflammatory responses in this model. Immunohistochemical detection of MMP-9 in murine neutrophils during peak acute inflammatory responses also supports this assertion (Fig. 6). In addition, production of dimeric MMP-9 production and the detection of monomer MMP-9 coincident with the onset and during the peak of acute inflammation at days 4 to 10 postinfection as shown in Fig. 4A, B, E, and F also support the role of neutrophils as a primary source of MMP-9 during time points previously shown to coincide with peak acute inflammation. The appearance of higher levels of monomeric MMP-9 gelatinolytic activity early in response to infection in the C3H/HeN strain (Fig. 3 and 4, days 7 through 14) likely correlates with the more vigorous acute inflammatory infiltrate in this strain during this same time frame (7, 39). In addition to day 14, shown herein, immunohistochemical results for MMP-9-specific staining indicate that neutrophils are a significant source of MMP-9 beginning at day 4 and through days 17 to 21 postinfection (data not shown). Lastly, while both monomeric and homodimeric forms of MMP-9 were observed throughout the infection in the C57BL/6 mice, only monomeric MMP-9 was observed to have consistent and significant activity on zymography. Beyond day 21 in the C3H/HeN strain, only homodimers of MMP-9 were observed and there was very little gelatinolytic activity associated with this form of the molecule on zymography.

In Fig. 4C and D, the lower-molecular-mass band ($<$50 kDa) observed in reducing gels for Western blot analysis would also be consistent with the post-translational processing of MMP-9. In this regard, the plasminogen activator/plasmin system and other MMPs such as MMP-1, MMP-3, MMP-10, and MMP-13 can regulate the activity of MMP-9 (14, 45). In some cases, this processing converts proMMP-9 to a more active but slightly lower-molecular-mass form via cleavage of a 5-amino-acid segment of the proMMP-9 molecule. In other instances, MMP-9 is cleaved to an inactive form in the same molecular mass range seen in Fig. 4C and D. Interestingly, we observed that transcription of the genes for several of these MMP-9 coregulating MMPs was enhanced in response to infection (Table 1), particularly in the C3H/HeN strain. On Western blots, monomer MMP-9 was observed in both strains of mice but appeared earlier in the infection course and was more abundant in the C3H/HeN strain. In light of the findings that monomeric

MMP-9 is more active than dimeric forms (45), we interpret these observations to indicate an abundance of active MMP-9 earlier in response to infection in the C3H/HeN mice than the C57BL/6 mice. However, as the infection resolves (day 21 and beyond), the C57BL/6 mice appear to produce a more monomeric form of the molecule and less conversion to the putative inactive low-molecular-mass form. This could be at least one event that influences the differences in epithelial dissolution and the resulting ECM accumulation and fibrosis between these two strains. Whether these observations may ultimately be linked to the observed differing disease outcomes in these two strains of mice is not clear at this time.

Another point of regulation for MMP-9 is the availability of TIMP-1. While we did not directly assess TIMP activity on MMP-9 in our experiments, we did find enhanced TIMP-1 gene expression through day 21 in the C3H/HeN mice. The activity of MMP-9 derived from any cell type may be regulated by the availability and concentration of TIMP-1 in the extracellular matrix (reviewed in reference 45). Most cells (e.g., macrophages and cells of mesenchymal origin) synthesize MMP-9 in stoichiometric balance with TIMP-1. Neutrophils, which are abundant for the first 14 days of this infection, particularly in the oviducts of the susceptible strain (45), presynthesize MMP-9 sans TIMP-1 (45). Another related point of regulation of MMP-9 activity could be the degree of glycosylation. Western blot results presented herein imply at least four molecular mass species of MMP-9 monomers in the C57BL/6 mice compared to C3H/HeN mice. Possessing at least three glycosylation sites, these bands could represent various degrees of glycosylation ranging from full glycosylation to unglycosylated MMP-9 (45). The degree of glycosylation of MMP-9 may affect its catalytic capacity by altering its ability to associate with TIMP-1 (47). Thus, if a role for MMP-9 in pathogenesis is hypothesized, multiple factors other than mere excessive production may be involved.

Given its predilection for degrading type IV collagen, which is critical in anchoring epithelial cells to the basal lamina of mucosal epithelium, we hypothesize that excessive MMP-9 activity could account for the epithelial dissolution early in the infection (7, 39, 40). This hypothesis is supported by concurrent collagen IV derangement with the presence of MMP-9-producing neutrophils (33). Perhaps a protective role for moderate MMP-9 activity later in response to the infection could be postulated for the resistant strain due to the evidence of more MMP-9 activity in this strain during the time frame of infection resolution and tissue repair (Fig. 2 and 3) (see also reference 39). In this regard, a sustained but moderate MMP-9 activity could prevent excessive ECM accumulation and fibrosis in the resistant strain. Other than epithelial dissolution and damage, roles for MMP-9 and other MMPs that have potential consequences on pathological processes include the proteolytic modification of chemokines and inflammatory cytokines (15, 30, 46, 48) and proteolysis-facilitated extravasation, chemotaxis, and the transepithelial migration of inflammatory cells (18, 30, 44, 45). Thus, it is not difficult to envision the involvement of MMP on multiple levels in the pathogenesis of this infection. The exact influence of MMP on pathogenesis in this model will require careful examination of MMP knockout systems and the use of selective chemical inhibitors of MMP activity in vivo and the implementation of more controlled systems in vitro.

ACKNOWLEDGMENTS

We thank the excellent contribution of Angelo Izzo for his original suggestion of exploring the role of MMP in chlamydia and advice on accessing their activity. We also thank Linda Izzo for her initial technical assistance with the zymography assays.

This work was supported by Public Health Service grant no. AI49354 to K.H.R.

REFERENCES

1. **Abu el-Asrar, A. M., K. Geboes, S. A. Al Kharashi, A. A. Al Mosallam, L. Missotten, L. Paemen, and G. Opdenakker.** 2000. Expression of gelatinase B in trachomatous conjunctivitis. Br. J. Ophthalmol. **84:**85–91.
2. **Abu el-Asrar, A. M., K. Geboes, and L. Missotten.** 2001. Immunology of trachomatous conjunctivitis. Bull. Soc. Belge Ophtalmol. **2001:**73–96.
3. **Ault, K. A., K. A. Kelly, P. E. Ruther, A. A. Izzo, L. S. Izzo, I. M. Sigar, and K. H. Ramsey.** 2002. *Chlamydia trachomatis* enhances the expression of matrix metalloproteinases in an in vitro model of the human fallopian tube infection. Am. J. Obstet. Gynecol. **187:**1377–1383.
4. **Byrne, G. I., M. Padilla, D. Lacey, D. Paulnock, and L. G. Xiu.** 1990. Mouse model for protective immunity to chlamydia, p. 236–240. *In* W. R. Bowie, H. D. Caldwell, R. P. Jones, P. A. Mardh, G. L. Ridgway, J. Schachter, W. E. Stamm, and M. E. Ward (ed.), Chlamydial infections. Proceedings of the Seventh International Symposium on Human Chlamydial Infections. Cambridge University Press, Cambridge, United Kingdom.
5. **Cotter, T. W., G. S. Miranpuri, K. H. Ramsey, C. E. Poulsen, and G. I. Byrne.** 1997. Reactivation of chlamydial genital tract infection in mice. Infect. Immun. **65:**2067–2073.
6. **Cotter, T. W., K. H. Ramsey, G. S. Miranpuri, C. E. Poulsen, and G. I. Byrne.** 1997. Dissemination of *Chlamydia trachomatis* chronic genital tract infection in gamma interferon gene knockout mice. Infect. Immun. **65:**2145–2152.
7. **Darville, T., C. W. Andrews, K. K. Laffoon, W. Shymasani, L. R. Kishen, and R. G. Rank.** 1997. Mouse strain-dependent variation in the course and outcome of chlamydial genital tract infection is associated with differences in host response. Infect. Immun. **65:**3065–3073.
8. **Darville, T., C. W. Andrews, Jr., and R. G. Rank.** 2000. Does inhibition of tumor necrosis factor alpha affect chlamydial genital tract infection in mice and guinea pigs? Infect. Immun. **68:**5299–5305.
9. **Darville, T., C. W. Andrews, Jr., J. D. Sikes, P. L. Fraley, and R. G. Rank.** 2001. Early local cytokine profiles in strains of mice with different outcomes from chlamydial genital tract infection. Infect. Immun. **69:**3556–3561.
10. **Darville, T., J. M. O'Neill, C. W. Andrews, Jr., U. M. Nagarajan, L. Stahl, and D. M. Ojcius.** 2003. Toll-like receptor-2, but not Toll-like receptor-4, is essential for development of oviduct pathology in chlamydial genital tract infection. J. Immunol. **171:**6187–6197.
11. **De La Maza, L. M., S. Pal, A. Khamesipour, and E. M. Peterson.** 1994. Intravaginal inoculation of mice with the *Chlamydia trachomatis* mouse pneumonitis biovar results in infertility. Infect. Immun. **62:**2094–2097.
12. **Descamps, F. J., P. E. Van den Steen, I. Nelissen, J. Van Damme, and G. Opdenakker.** 2003. Remnant epitopes generate autoimmunity: from rheumatoid arthritis and multiple sclerosis to diabetes. Adv. Exp. Med. Biol. **535:**69–77.
13. **Dessus-Babus, S., S. T. Knight, and P. B. Wyrick.** 2000. Chlamydial infection of polarized HeLa cells induces PMN chemotaxis but the cytokine profile varies between disseminating and non-disseminating strains. Cell. Microbiol. **2:**317–327.
14. **Dreier, R., S. Grassel, S. Fuchs, J. Schaumburger, and P. Bruckner.** 2004. Pro-MMP-9 is a specific macrophage product and is activated by osteoarthritic chondrocytes via MMP-3 or a MT1-MMP/MMP-13 cascade. Exp. Cell Res. **297:**303–312.
15. **Gearing, A. J., P. Beckett, M. Christodoulou, M. Churchill, J. M. Clements, M. Crimmin, A. H. Davidson, A. H. Drummond, W. A. Galloway, and R. Gilbert.** 1995. Matrix metalloproteinases and processing of pro-TNF-alpha. J. Leukoc. Biol. **57:**774–777.
16. **Hestdal, K., F. W. Ruscetti, J. N. Ihle, S. E. Jacobsen, C. M. Dubois, W. C. Kopp, D. L. Longo, and J. R. Keller.** 1991. Characterization and regulation of RB6-8C5 antigen expression on murine bone marrow cells. J. Immunol. **147:**22–28.
17. **Huang, J., F. J. DeGraves, S. D. Lenz, D. Gao, P. Feng, D. Li, T. Schlapp, and B. Kaltenboeck.** 2002. The quantity of nitric oxide released by macrophages regulates *Chlamydia*-induced disease. Proc. Natl. Acad. Sci. USA **99:**3914–3919.
18. **Huber, D., M. S. Balda, and K. Matter.** 1998. Transepithelial migration of neutrophils. Invasion Metastasis **18:**70–80.
19. **Imai, K., Y. Yokohama, I. Nakanishi, E. Ohuchi, Y. Fujii, N. Nakai, and Y. Okada.** 1995. Matrix metalloproteinase 7 (matrilysin) from human rectal carcinoma cells. Activation of the precursor, interaction with other matrix metalloproteinases and enzymic properties. J. Biol. Chem. **270:**6691–6697.

20. **Ito, A., A. Mukaiyama, Y. Itoh, H. Nagase, I. B. Thogersen, J. J. Enghild, Y. Sasaguri, and Y. Mori.** 1996. Degradation of interleukin 1beta by matrix metalloproteinases. J. Biol. Chem. **271:**14657–14660.
21. **Johnson, L. L., R. Dyer, and D. J. Hupe.** 1998. Matrix metalloproteinases. Curr. Opin. Chem. Biol. **2:**466–471.
22. **Karagiannis, E. D., and A. S. Popel.** 2004. A theoretical model of type I collagen proteolysis by matrix metalloproteinase (MMP) 2 and membrane type 1 MMP in the presence of tissue inhibitor of metalloproteinase 2. J. Biol. Chem. **279:**39105–39114.
23. **Kumar, R., K. Xie, I. Eue, Z. Dong, J. J. Killion, and I. J. Fidler.** 2000. Differential regulation of type IV collagenases and metalloelastase in murine macrophages by the synthetic bacterial lipopeptide JBT 3002. Int. J. Immunopharmacol. **22:**431–443.
24. **Luo, Y., and M. E. Dorf.** 1997. In vitro assays for leuckocyte function—isolation of mouse neutrophils, p. 3.20.1–3.20.6. *In* J. E. Coligan, A. M. Kruisbeek, D. H. Margulies, E. M. Shevach, and W. Strober (ed.), Current protocols in immunology. John Wiley & Sons, Inc., New York, N.Y.
25. **Masure, S., L. Paemen, A. Van, I., P. Fiten, P. Proost, A. Billiau, J. Van Damme, and G. Opdenakker.** 1997. Production and characterization of recombinant active mouse gelatinase B from eukaryotic cells and in vivo effects after intravenous administration. Eur. J. Biochem. **244:**21–30.
26. **Mayer, A. M., S. Oh, K. H. Ramsey, P. B. Jacobson, K. B. Glaser, and A. M. Romanic.** 1999. *Escherichia coli* lipopolysaccharide potentiation and inhibition of rat neonatal microglia superoxide anion generation: correlation with prior lactic dehydrogenase, nitric oxide, tumor necrosis factor-alpha, thromboxane B2, and metalloprotease release. Shock **11:**180–186.
27. **McQuibban, G. A., J. H. Gong, E. M. Tam, C. A. McCulloch, I. Clark-Lewis, and C. M. Overall.** 2000. Inflammation dampened by gelatinase A cleavage of monocyte chemoattractant protein-3. Science **289:**1202–1206.
28. **Meli, D. N., S. Christen, and S. L. Leib.** 2003. Matrix metalloproteinase-9 in pneumococcal meningitis: activation via an oxidative pathway. J. Infect. Dis. **187:**1411–1415.
29. **Nagase, H. and J. F. Woessner, Jr.** 1999. Matrix metalloproteinases. J. Biol. Chem. **274:**21491–21494.
30. **Opdenakker, G., P. E. Van den Steen, B. Dubois, I. Nelissen, E. Van Coillie, S. Masure, P. Proost, and J. Van Damme.** 2001. Gelatinase B functions as regulator and effector in leukocyte biology. J. Leukoc. Biol. **69:**851–859.
31. **Peppin, G. J., and S. J. Weiss.** 1986. Activation of the endogenous metalloproteinase, gelatinase, by triggered human neutrophils. Proc. Natl. Acad. Sci. USA **83:**4322–4326.
32. **Perfettini, J. L., D. M. Ojcius, C. W. Andrews, Jr., S. J. Korsmeyer, R. G. Rank, and T. Darville.** 2003. Role of proapoptotic BAX in propagation of *Chlamydia muridarum* (the mouse pneumonitis strain of *Chlamydia trachomatis*) and the host inflammatory response. J. Biol. Chem. **278:**9496–9502.
33. **Ramsey, K. H., J. H. Schripsema, I. M. Sigar, A. A. Shah, M. T. Imtiaz, J. N. Kasimos, and S. Inouye.** 2004. Histological assessment of extracellular matrix modification as a consequence of chlamydial urogenital infection of mice, p. 372. *In* J. Deak (ed.), Proceedings of the 5th Meeting of the European Society for Chlamydia Research. University of Szged, Budapest, Hungary.
34. **Ramsey, K. H., T. W. Cotter, R. D. Salyer, G. S. Miranpuri, M. A. Yanez, C. E. Poulsen, J. L. DeWolfe, and G. I. Byrne.** 1999. Prior genital tract infection with a murine or human biovar of *Chlamydia trachomatis* protects mice against heterotypic challenge infection. Infect. Immun. **67:**3019–3025.
35. **Ramsey, K. H., G. S. Miranpuri, I. M. Sigar, S. Ouellette, and G. I. Byrne.** 2001. *Chlamydia trachomatis* persistence in the female mouse genital tract: inducible nitric oxide synthase and infection outcome. Infect. Immun. **69:** 5131–5137.
36. **Ramsey, K. H., I. M. Sigar, S. V. Rana, J. Gupta, S. M. Holland, and G. I. Byrne.** 2001. Role for inducible nitric oxide synthase in protection from chronic *Chlamydia trachomatis* urogenital disease in mice and its regulation by oxygen free radicals. Infect. Immun. **69:**7374–7379.
37. **Reynolds, J. J.** 1996. Collagenases and tissue inhibitors of metalloproteinases: a functional balance in tissue degradation. Oral Dis. **2:**70–76.
38. **Ries, C., and P. E. Petrides.** 1995. Cytokine regulation of matrix metalloproteinase activity and its regulatory dysfunction in disease. Biol. Chem. Hoppe-Seyler **376:**345–355.
39. **Shah, A. A., J. H. Schripsema, M. T. Imtiaz, I. M. Sigar, J. Kasimos, P. G. Matos, S. Inouye, and K. H. Ramsey.** 2005. Histopathologic changes related to fibrotic oviduct occlusion after genital tract infection of mice with *Chlamydia muridarum*. Sex Transm. Dis. **32:**49–56.
40. **Swenson, C. E., E. Donegan, and J. Schachter.** 1983. *Chlamydia trachomatis*-induced salpingitis in mice. J. Infect. Dis. **148:**1101–1107.
41. **Tanaka, H., K. Hojo, H. Yoshida, T. Yoshioka, and K. Sugita.** 1993. Molecular cloning and expression of the mouse 105-kDa gelatinase cDNA. Biochem. Biophys. Res. Commun. **190:**732–740.
42. **Toth, M., I. Chvyrkova, M. M. Bernardo, S. Hernandez-Barrantes, and R. Fridman.** 2003. Pro-MMP-9 activation by the MT1-MMP/MMP-2 axis and MMP-3: role of TIMP-2 and plasma membranes. Biochem. Biophys. Res. Commun. **308:**386–395.
43. **Tuffrey, M., F. Alexander, C. Woods, and D. Taylor-Robinson.** 1992. Genetic susceptibility to chlamydial salpingitis and subsequent infertility in mice. J. Reprod. Fertil. **95:**31–38.
44. **Vaday, G. G., and O. Lider.** 2000. Extracellular matrix moieties, cytokines, and enzymes: dynamic effects on immune cell behavior and inflammation. J. Leukoc. Biol. **67:**149–159.
45. **Van den Steen, P. E., B. Dubois, I. Nelissen, P. M. Rudd, R. A. Dwek, and G. Opdenakker.** 2002. Biochemistry and molecular biology of gelatinase B or matrix metalloproteinase-9 (MMP-9). Crit. Rev. Biochem. Mol. Biol. **37:** 375–536.
46. **Van den Steen, P. E., S. J. Husson, P. Proost, J. Van Damme, and G. Opdenakker.** 2003. Carboxyterminal cleavage of the chemokines MIG and IP-10 by gelatinase B and neutrophil collagenase. Biochem. Biophys. Res. Commun. **310:**889–896.
47. **Van den Steen, P. E., G. Opdenakker, M. R. Wormald, R. A. Dwek, and P. M. Rudd.** 2001. Matrix remodelling enzymes, the protease cascade and glycosylation. Biochim. Biophys. Acta **1528:**61–73.
48. **Van den Steen, P. E., A. Wuyts, S. J. Husson, P. Proost, J. Van Damme, and G. Opdenakker.** 2003. Gelatinase B/MMP-9 and neutrophil collagenase/MMP-8 process the chemokines human GCP-2/CXCL6, ENA-78/CXCL5 and mouse GCP-2/LIX and modulate their physiological activities. Eur. J. Biochem. **270:**3739–3749.
49. **Visse, R., and H. Nagase.** 2003. Matrix metalloproteinases and tissue inhibitors of metalloproteinases: structure, function, and biochemistry. Circ. Res. **92:**827–839.
50. **Ward, M. E.** 1999. Mechanisms of chlamydia-induced disease, p. 171–210. *In* R. S. Stephens (ed.), *Chlamydia*: intracellular biology, pathogenesis, and immunity. ASM Press, Washington, D.C.
51. **Weiss, S. J.** 1989. Tissue destruction by neutrophils. N. Engl. J. Med. **320:** 365–376.
52. **Weiss, S. J., and G. J. Peppin.** 1986. Collagenolytic metalloenzymes of the human neutrophil. Characteristics, regulation and potential function in vivo. Biochem. Pharmacol. **35:**3189–3197.
53. **Williams, D. M., J. Schachter, J. J. Coalson, and B. Grubbs.** 1984. Cellular immunity to mouse pneumonitis agent. J. Infect. Dis. **149:**630–639.
54. **Wyrick, P. B., S. T. Knight, T. R. Paul, R. G. Rank, and C. S. Barbier.** 1999. Persistent chlamydial envelope antigens in antibiotic-exposed infected cells trigger neutrophil chemotaxis. J. Infect. Dis. **179:**954–966.

Editor: F. C. Fang